FINE-SCALE PRECIPITATION IN Al ALLOY 6061

G.A. Edwards[1], G.L.Dunlop[1] and M.J. Couper[2]
1. CRC for Alloy and Solidification Technology (CAST), Department of Mining and Metallurgical Engineering, The University of Queensland, St. Lucia, Queensland, AUSTRALIA 4072.
2. Comalco Research Centre, 15 Edgars Rd., Thomastown, Victoria, AUSTRALIA 3074.

Abstract

Fine-scale precipitation in Al alloy 6061 has been studied with differential scanning calorimetry (DSC), atom probe field ion microscopy (APFIM) and transmission electron microscopy (TEM). It was found that the precipitation sequence was: independent clusters of Mg and Si atoms → co-clusters that contained Mg and Si atoms → small precipitates of unknown structure → β'' needle-shaped precipitates → B' lath-shaped precipitates and some β' rod-shaped precipitates. A new structure is proposed for β'': base-centred monoclinic, a = 15.34Å, b = 4.05Å, c = 6.89Å, β = 106°. The results are compared with previous studies in the literature.

Introduction

Precipitation in Al-Mg-Si alloys has been extensively studied but many details of the precipitation sequence remain the subject of controversy. In a recent study [1] it was proposed that the precipitation sequence was: clusters of Si atoms → GP-I zones → GP-II zones/β'' → β' → Mg_2Si. There is disagreement in the literature concerning several of these stages. For the initial, 'pre-precipitation' stages, it has been variously proposed that clustering of Mg atoms [2], co-clustering of Mg and Si atoms [2-4], formation of Mg-vacancy clusters [2], and the formation of vacancy-vacancy clusters [2] may occur. Dilute Al-Si alloys do not exhibit the same thermal effects [2] or changes in resistance [4] that have been observed for Al-Mg-Si alloys. This suggests that a process other than clustering of Si atoms occurs in the early stages of ageing in Al-Mg-Si alloys. The nature of the GPI zones is also unclear. Lutts [5] found that these precipitates had no clear structure, and contained a significant quantity of vacancies. However Cordier and Gruhl [6] and Dutta et al.[1] proposed that the precipitates were GP zones. Several different structures have also been proposed for β'' [7-9]. The structure of β' has been determined [9] and confirmed by subsequent high resolution and microdiffraction work [8,10]. However another intermediate precipitate, B', has also been observed in Al-Mg-Si alloys [11] and the quantity of this phase has been found to increase with increasing Si content [10].

In this paper the results of an extensive investigation into precipitation in Al alloy 6061 are presented.

Experimental

Al alloy 6061 was supplied by Comalco Research Centre in the form of as-extruded bar. The composition of the alloy was: 0.80Mg, 0.79Si, 0.18Cu, 0.22Fe, 0.01Ti. DSC was carried out on

a Perkin-Elmer DSC7 instrument, using a heating rate of 5°C per minute. Specimens for DSC were solution treated for 1.5h at 530°C in an argon atmosphere, and then quenched into iced water. DSC scanning commenced within 10 minutes of quenching. The specimens weighed ~ 59mg. Thin-foil specimens for TEM were prepared by electropolishing in a nitric acid:methanol 1:4 solution, at -30°C and ~8V, using a Tenupol jet polisher. Transmission electron microscopy was performed using JEOL 4000FX and 1210 instruments, operating at 400kV and 120kV respectively. High resolution dark-field electron microscopy (HRDEM) was used to image the crystal structures of individual fine-scale precipitates. This technique is further described elsewhere [12].

Atom probe field ion microscopy was carried out at Chalmers University of Technology, Sweden. Details of the atom-probe instrument have been reported elsewhere [13]. APFIM data was obtained using a specimen temperature of about 25K, a pulse fraction of 20% and a vacuum of less than 1.5×10^{-10} mbar. These conditions were chosen to minimise DC evaporation or retention of atoms. Concentration profiles were derived from atoms collected from a cylinder of material approximately 16Å in diameter by maintaining the effective radius of the probe aperture at about 8Å. The profiles were plotted by dividing the data into groups of 75 or 100 ions, obtaining the numbers of solute atoms in each group and then plotting these numbers versus the total number of ions collected. The detector efficiency was kept constant during acquisition by varying the channel plate voltage [14].

Differential Scanning Calorimetry

DSC results for alloy 6061 are presented in Figure 1. The basic features of the curve, i.e. the number and positions of exothermic and endothermic peaks, agree with previous investigations [1,15]. The broadness and asymmetry of the initial exothermic peak suggest that this peak may be comprised of two overlapping peaks, in agreement with Gupta et al.[2]. However these peaks are not as clearly separated as those in the work by Gupta et al.. The second exothermic peak clearly consists of two overlapping peaks, as evidenced by the shoulder at the low temperature side of the peak. The third and fourth exothermic peaks appear to be similar to those in previous investigations [1,15].
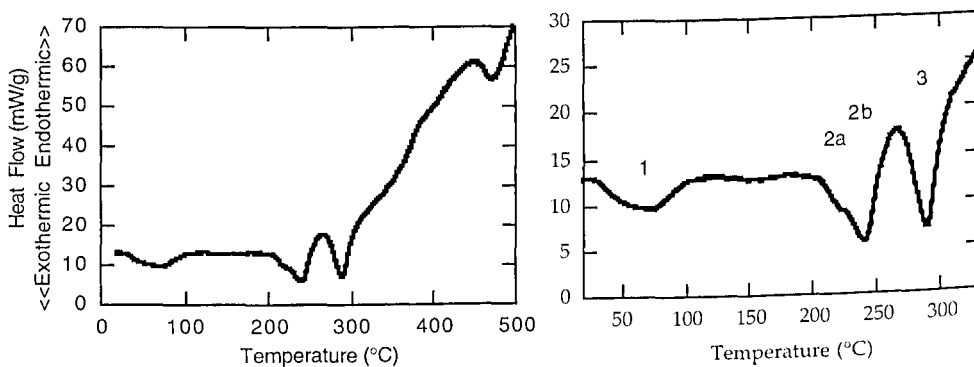

Figure 1. DSC results for alloy 6061 (displayed at two different temperature scales). The number and positions of exothermic and endothermic peaks are in agreement with previously reported results. The broadness and asymmetry of peak 1 suggests that it may be comprised of two overlapping peaks. Peak 2 clearly consists of two overlapping peaks, designated 2a and 2b.

As-Quenched Microstructure

Care must be taken when investigating fine-scale precipitation with TEM as preparation of the thin foils may introduce artefacts that may appear similar to fine-scale precipitates and which can produce faint diffraction effects [16]. For this reason, TEM analysis of as-quenched specimens, in which precipitation is obviously minimal, was carried out.

Figure 2 shows TEM bright and dark field micrographs and SADP (B = [001]$_{Al}$) from a specimen that was solution-treated, quenched and aged ~4h at room temperature. Minimal fine-scale contrast is apparent on the bright field image, however several faint reflections were present on the selected area diffraction patterns (SADPs). Dark field micrographs that were obtained using these reflections showed some fine-scale contrast (Figure 2b) and a bright band at the edge of the foil. The intensity of the faint reflections decreased after ion-beam thinning the specimen, and increased for specimens that were clearly contaminated. Therefore it is believed that these reflections resulted from a layer of oxide or other material on the surface of the foils.
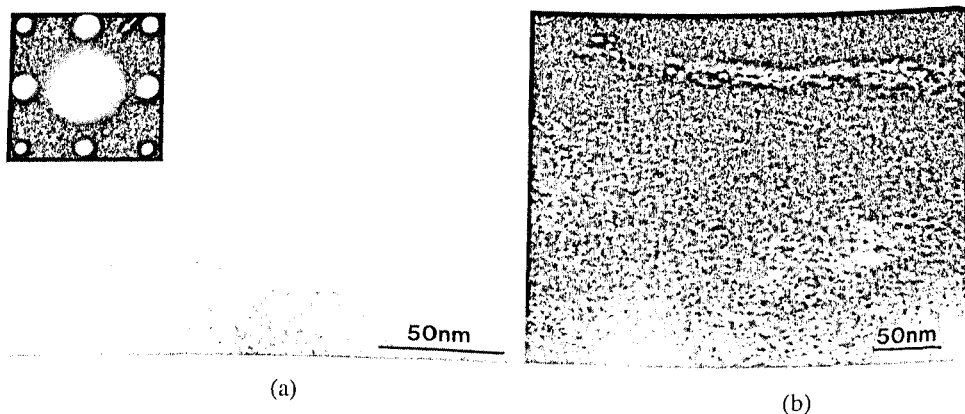

(a)   (b)

Figure 2. (a) Bright-field TEM micrograph and SADP, and (b) dark field TEM micrograph that was obtained using the arrowed reflection in (a) (B = [001]$_{Al}$). The faint reflections and the fine-scale contrast in the dark field micrographs are thought to arise from a layer of oxide or other contaminant that was on the surface of the foils.

Peak 1 in the DSC Scan

Specimens that were heated to 100°C at 5°C per minute were examined by TEM and APFIM. 100°C is close to the end of the first exothermic peak in the DSC scan. TEM bright and dark field micrographs and SADPs appeared to be·identical to those from the as-quenched specimens. However concentration profiles that were obtained with the atom probe showed the presence of three different types of clusters of atoms: clusters of Mg atoms, clusters of Si atoms, and co-clusters that contained both Mg and Si atoms (Figure 3). This result is in agreement with previous APFIM results for isothermal ageing at 70°C [17], where it was shown that independent clusters of Mg and Si atoms formed first, and this was followed by co-clustering of the Mg and Si atoms.
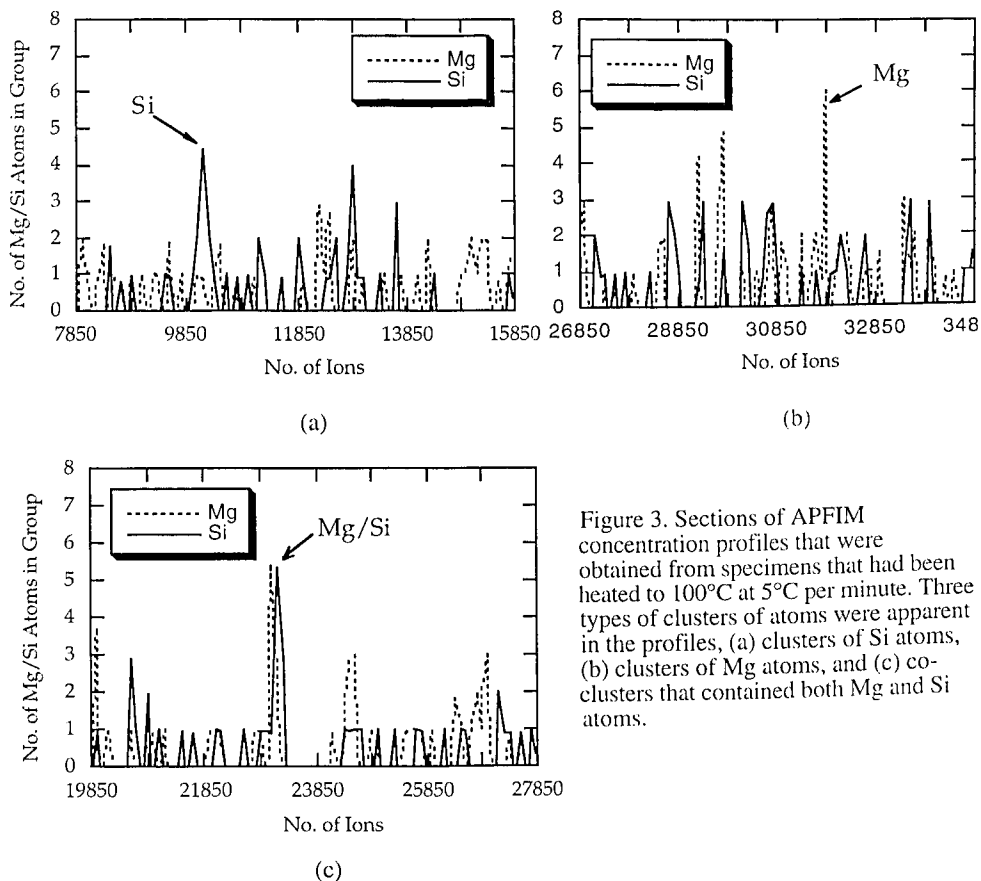
(a)

(b)

(c)

Figure 3. Sections of APFIM concentration profiles that were obtained from specimens that had been heated to 100°C at 5°C per minute. Three types of clusters of atoms were apparent in the profiles, (a) clusters of Si atoms, (b) clusters of Mg atoms, and (c) co-clusters that contained both Mg and Si atoms.

Peak 2a in the DSC Scan

Small precipitates were visible in TEM images of specimens that had been heated to 215°C at 5°C per minute (Figure 4). This temperature is close to the shoulder of the second exothermic peak in the DSC scan. Bright field images showed fine-scale contrast that probably arose from strain-fields associated with fine-scale precipitates. High resolution dark field images highlighted small precipitates, however no clear structure was visible in most of the precipitates. Structure was visible in some precipitates that appeared to be similar to that of β" (Figure 4b) (see subsequent section), indicating that some transformation to β" had already occurred at this stage, when the precipitates were very small. Only reflections that were ascribed to a layer of oxide or other material were observed on SADPs. The structure of the small precipitates could not be determined.
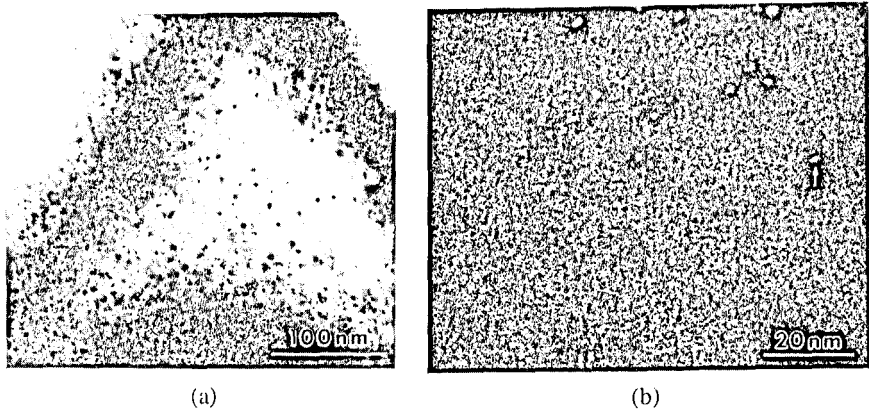
(a)	(b)

Figure 4. TEM micrographs (B = [001]$_{Al}$) from a specimen that was heated to 215°C at 5°C per minute. (a) Bright field micrograph and SADP, and (b) high resolution dark field micrograph. No clear structure was visible in most of the precipitates, however structure was visible in some precipitates that corresponded to the structure of β" (arrowed).

Peak 2b in the DSC Scan

Specimens that had been heated to 250°C at 5°C per minute contained needle-shaped precipitates that were clearly delineated by strain-field contrast (Figure 5a). SADPs taken with B = [001]$_{Al}$ contained streaks and some faint, circular reflections in addition to the oxide reflections from the oxide layer (Figure 5b). The appearance of the precipitates, and the streaks on the SADPs, are in agreement with previous observations for β" precipitates [18].

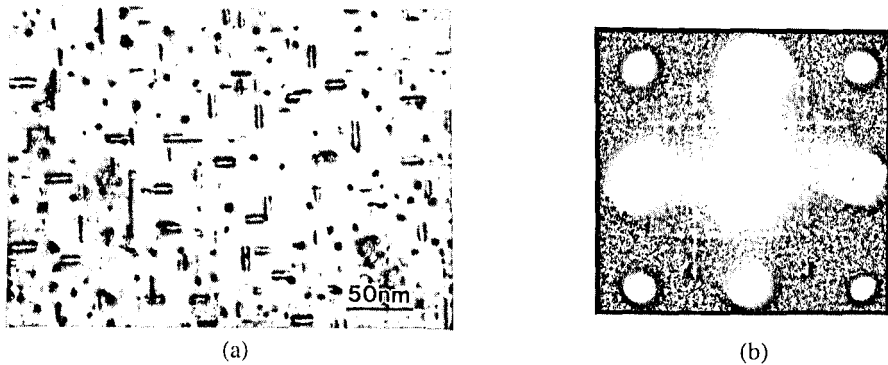| (a)	(b)

Figure 5. (a) Bright field TEM micrograph and (b) SADP from a specimen that had been heated at 5°C per minute to 250°C. Needle-shaped precipitates are visible via strain field contrast in (a). The SADP contained streaks and some faint, circular reflections in addition to the reflections from the oxide layer.

High resolution images were only obtained from precipitates that were aligned parallel to the electron beam. For other precipitate orientations, the small cross sectional diameters of the needle-shaped precipitates meant that there was generally overlap between the Al matrix and the precipitates. Hence only one view of the precipitate lattice could be obtained (Figure 6). The high

resolution images showed that the precipitate lattice had a periodicity that is defined by the vectors a_1 and c in Figure 6. A detailed analysis of the high resolution images, the streaks in SADPs and the faint, circular reflections in SADPs led to a base-centred monoclinic structure, a = 15.34 ± 0.12Å, b = 4.05 Å, c = 6.83 ± 0.15 Å, β = 106° ± 1.5° [19]. The vector a is twice the length of the vector a_1 in Figure 6. The orientation relationship between this structure and the Al lattice was: $(001)_{Al} // (010)_{\beta''}$, $[310]_{Al} // [001]_{\beta''}$. There are twelve equivalent orientations of the precipitate, four for each $<001>_{Al}$ orientation of the needle axes. The precipitate structure is fully coherent with the Al matrix, and there is significant misfit along both sides of the rhombohedral cross-section of the precipitate. There is negligible misfit along the length of the precipitates. Calculated misfits are in agreement with the observed strain-field contrast [19].
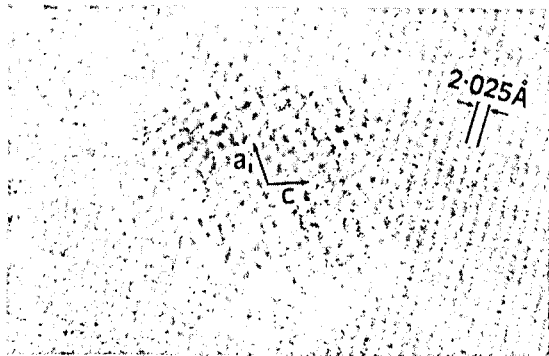

Figure 6. High resolution micrograph of a β" precipitate whose axis was aligned with the electron beam ($[001]_{Al}$). The lattice has a periodicity that can be described with the vectors a_1 and c.

Peak 3 in the DSC Scans

Specimens that had been heated to 320°C at 5°C per minute contained lath-shaped precipitates that were aligned along $<001>_{Al}$ directions (Figure 7). The precipitates were substantially longer than those in Figure 6. Most precipitates had rectangular cross sections (Figure 8a). A small number of precipitates had more equiaxed cross-sections (Figure 8b). The high resolution images of the more equiaxed precipitates showed a hexagonal periodicity, the spacing of which (a = 7.01Å) corresponds to that of β' [9]. The periodicity in dark-field images of the precipitates with rectangular cross sections corresponded to that of B' (hexagonal, a = 10.4Å, c=4.05Å) (Figure 9a). This periodicity was not immediately obvious in bright field images of this precipitate, however Fourier transforms from the images showed arrangements of reflections that matched the structure and orientation of B'(Figure 9b).

Discussion

Three types of clusters of atoms were present in specimens that had been heated to the end of the first exothermic DSC peak. However not all three types necessarily formed during the exothermic peak. It is possible that some clustering of atoms occurred during quenching from the solution treatment temperature, or immediately after quenching, prior to the DSC analysis. DSC results for Al-Si alloys do not show a low temperature exothermic peak, and there is evidence to suggest that clusters of Si atoms form extremely rapidly after quenching in Al-Si alloys [20]. Therefore it is thought that the exothermic peak in the DSC scan may have resulted from clustering of Mg atoms and co-clustering of both Mg and Si atoms.

The structure of the small precipitates of unknown structure is not known and is extremely difficult to determine. The fact that the precipitates were imaged in dark field indicates that there was some diffracted intensity from the precipitates. However this must have been too weak to be visible on
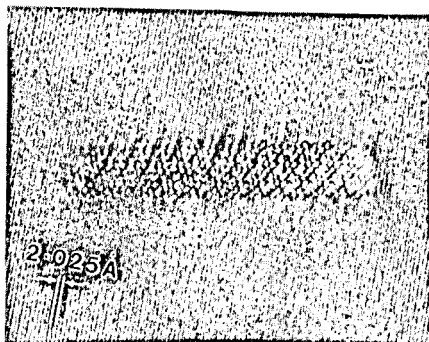
SADPs. It was found that these precipitates transform quickly to β", therefore it is thought that their main role in precipitation hardening is to nucleate β" precipitates.

The structure that was proposed for β" is different to those previously reported [7,8]. The precipitates analysed by Lynch et al. [8] formed in a different alloy to that used in the present investigation, and were significantly larger than the precipitates analysed here. Therefore the precipitate that was analysed by Lynch et al. may well have been a different precipitate to that analysed in this investigation. Shchergoleva [7] also used a different alloy, and used x-ray methods to determine the crystal structure. Given the difficulties experienced by other investigators who have used x-ray methods, the analysis by Shchergoleva must be viewed with caution.
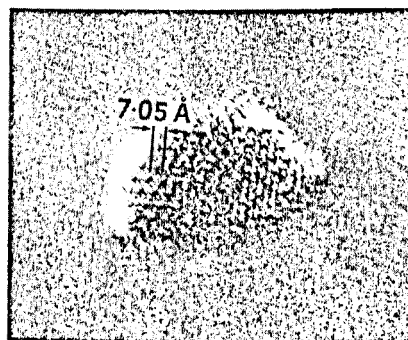
The simultaneous occurrence of both B' and β' precipitates is in agreement with previous results for isothermal ageing [10]. The predominance of the B' precipitate in this alloy is also in agreement with the work of Matsuda et al. [10]. In that investigation it was found that for alloys with 0.4% excess Si (the same amount of excess Si as the alloy in the present investigation), the predominant precipitate was B'. Some β' precipitates were also observed, in agreement with the present observations.

Figure 7. TEM bright field micrograph and SADP (B = [001]$_{Al}$) showing lath-shaped precipitates in a specimen that had been heated at 5°C per minute to 320°C, just beyond the third peak in the DSC scan.

(a)   (b)

Figure 8. High resolution electron micrographs of precipitates in Figure 7. (a) B' and (b) β'. The hexagonal lattice of B' was not obvious in bright field images, however it was apparent in dark field images and in Fourier transforms of the bright field image (Figure 9).

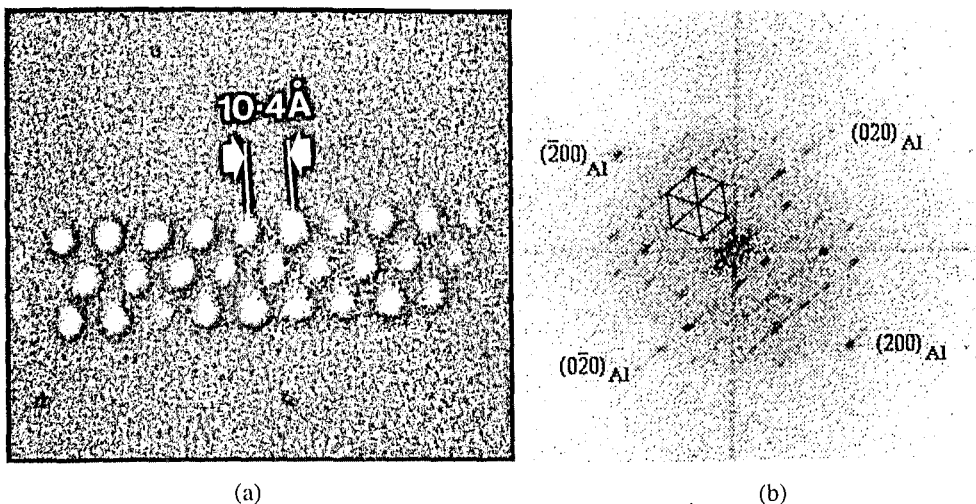(a)   (b)

Figure 9. (a) High resolution dark field image of a B' precipitate and (b) Fourier transformation of Figure 8a. The hexagonal periodicity of the B' structure is evident in both the dark field image and the Fourier transform.

References

1. I. Dutta and S.M. Allen, J. Materials Science Letters, 10, (1991), 323.
2. A.K. Gupta and D.J. Lloyd, Aluminium Alloys: Their Physical and Mechanical Properties, Vol. 2, Eds. L. Arnberg et al., Norwegian Inst. of Technology and SINTEF Metallurgy, Trondheim, 1992), 21.
3. I. Kovacs, J. Lendvai, E. Nagy, Acta Metallurgica, 20, (1972), 975.
4. D.K. Chatterjee & K.M Entwhistle, J. Institute of Metals, 101, (1973), 53.
5. A. Lutts, Acta Metallurgica, 9, 1961, 577.
6. H. Cordier and W. Gruhl, Zeitschrift Fur Metallkunde, Bd. 56, H.10, (1965), 669.
7. T.V. Shchegoleva, Physics of Metals and Metallography, 25, (1968), 56.
8. J.P. Lynch, L.M. Brown and M.H. Jacobs, Acta Metallurgica, 30, (1982), 1389.
9. M.H. Jacobs, Philosophical Magazine, 26, 1972, 1.
10. K. Matsuda, Y. Uetani, H. Anada, S. Tada, S. Ikeno, Aluminium Alloys: Their Physical and Mechanical Properties, Vol. 1, Eds. L. Arnberg et al., (Norwegian Inst. of Technology and SINTEF Metallurgy, Trondheim, 1992,), 220.
11. S.D. Dumolt, D.E. Laughlin and J.C. Williams, Scripta Metallurgica, 18, 1984, 1347.
12. G.A. Edwards, M.J. Couper and G.L. Dunlop, this proceedings.
13. H-O Andren, J. Physics, 47, (1986), C7-483.
14. L. Lundin and U. Rolander, Applied Surface Science, 67, (1993), 459.
15. J.M. Papazian, Met.allurgical Transactions, 19A, (1988), 2953.
16. G. Thomas and M. Goringe, Transmission Electron Microscopy of Materials, (New York, John Wiley and Sons Inc., 1979).
17. G.A. Edwards, K. Stiller and G.L. Dunlop, Applied Surface Science, 76/77, (1994), 219.
18. G. Thomas, J. Institute of Metals, 90, (1961-62), 57.
19. G.A. Edwards, G.L. Dunlop and M.J. Couper, to be published.
20. E. Ozawa and H. Kimura, Materials Science and Engineering, 8, (1971), 327.